

Sodium-induced $2 \times 1 \rightarrow 1 \times 1$ surface structural transition on Si(111)

B. Reihl,* S. L. Sorensen,† R. Dudde,‡ and K. O. Magnusson§

IBM Research Division, Zurich Research Laboratory, CH-8803 Rüschlikon, Switzerland

(Received 16 March 1992)

Sodium deposited on the cleaved Si(111) 2×1 surface induces a $2 \times 1 \rightarrow 1 \times 1$ surface structural transition at about $\frac{1}{2}$ monolayer coverage. Angle-resolved direct and inverse photoemission reveal the surface to be semiconducting. The measured energy dispersion of the empty Na-induced surface state is only consistent with calculations that favor the threefold-hollow site for the Na adsorption position. Its bonding character (ionic versus covalent) will be discussed.

The bonding character (ionic versus covalent) of alkali metals on semiconductor surfaces is controversial. This concerns the amount of charge transfer and the question where a possible metallization takes place, i.e., within the alkali-metal overlayer or the semiconductor substrate. For Cs on GaAs(110), recent electron-energy-loss spectroscopy¹ and scanning tunneling microscopy² studies have revealed a complex growth behavior determining the development of the surface electronic structure with a semiconductor-to-metal transition as a function of Cs coverage. Direct and inverse photoemission³ had identified Cs-induced empty surface states moving towards the Fermi level with increasing coverage, causing the metallization.

For silicon and its many possible surface reconstructions, the situation is more involved, since semiconductor atom rearrangements with coverage add to the complexity of the alkali-metal growth mechanism. Theoretical calculations for alkali-metal adsorption on silicon make predictions about the stability of the reconstructed surfaces with respect to alkali-metal deposition. The character of the bonding is the central question. Two extreme pictures may be used to describe the situation: (i) In the case of complete charge transfer of the alkali-metal valence s electron to the semiconductor surface the bonding is *ionic*, and the surface metallization as a function of coverage is caused by a partial filling of the silicon surface-state bands.⁴⁻⁷ The strong dipole field created by the positive alkali-metal ion and the negative image charge are causing the strong work-function reduction. (ii) In the other case charge transfer is fractional, and rather small, and a weak *covalent* bonding explains the work-function change by a polarization-dependent interaction.⁸⁻¹⁰ The metallization occurs within the alkali-metal overlayer as soon as the valence electron orbitals can overlap as a function of coverage, hence a critical surface atom density is required for metallization in contrast to the ionic-bonding picture. Some theories^{11,12} also favor a mixed type of bonding, i.e., almost ionic at low coverage, while the covalent character increases with coverage.

A common belief expressed in the literature is the equivalency and isoelectronic behavior of the different alkali-metal atoms, and in particular of potassium and cesium. Often, calculations performed for potassium are compared to experiments with cesium and vice versa.

For example, electronic-structure calculations for Si(111) 2×1 -K were compared⁴ to photoemission results of Cs on the same surface. Later, it was deduced from self-consistent total-energy calculations⁶ that the 2×1 surface reconstruction is unstable against K adsorption, favoring a 1×1 structure which may become insulating at higher coverages.⁶ Experimentally, however, it is cesium which destroys the 2×1 reconstruction yielding¹³ a new $\sqrt{3} \times \sqrt{3} R 30^\circ$ low-energy-electron-diffraction (LEED) pattern, while K leaves the 2×1 surface intact.¹⁴ The work-function reduction for both overlayer surfaces was found to be $\Delta\phi_{\text{sat}} \simeq -3.5$ eV, while theory⁴ predicted -1.6 eV. At this so-defined saturation coverage Si(111) $\sqrt{3} \times \sqrt{3} R 30^\circ$ -Cs is semiconducting, whereas the Si(111) 2×1 -K surface is metallic over a broad coverage regime¹⁴ with a filling of the Si π^* surface-state band in agreement with the ionic-bonding picture.⁴

Here we present our results for sodium deposition on the cleaved Si(111) 2×1 surface. As originally predicted⁶ for potassium, sodium now does induce a $2 \times 1 \rightarrow 1 \times 1$ surface structural transition, and angle-resolved direct and inverse photoemission spectroscopy reveal this surface to be semiconducting. We compare the measured energy dispersion of the occupied and empty Na-induced surface-state bands with existing electronic-structure calculations by Northrup⁵ favoring an ionic bonding and by Ossicini, Arcangeli, and Bisi¹⁰ supporting the covalent picture.

The apparatus¹⁵ was equipped with angle-resolved inverse and ultraviolet (direct) photoemission spectroscopy (IPS and UPS, respectively), Auger electron spectroscopy, and LEED. The IPS measurements were performed in the isochromat mode, detecting 9.5-eV photons. The electrostatically focused electron gun with BaO cathode had a beam divergence better than 4° , resulting in a resolution of the wave vector k_{\parallel} of $\Delta k_{\parallel} = 0.08 \text{ \AA}^{-1}$. The overall energy resolution (electrons and photons) was 0.35 eV in IPS and 0.1 eV in UPS employing He I radiation ($h\nu = 21.2$ eV) and a 180° hemispherical electron energy analyzer. The latter were derived from the width of the Fermi-level onset for a tantalum foil which could be interchanged with the silicon crystal. The position of the tantalum Fermi level was used as the energy reference, $E_F = 0$.

Single-crystalline bars of p -type doped silicon (resistivity $\rho \simeq 0.05 \text{ } \Omega \text{ cm}$) with a cross section of $5 \times 5 \text{ mm}^2$ were

cleaved along the $[\bar{2}11]$ direction, so that single-domain 2×1 reconstructed surfaces were produced and checked with LEED and UPS. Sodium was evaporated from a commercial getter source (SAES Getters, Italy) onto the sample at room temperature. The pressure during evaporation stayed in the low 10^{-10} -mbar range. The actual coverage was determined from the work-function change as determined by the diode method, i.e., by detecting the onset of the absorbed sample current from the electron gun.

Figure 1 shows the work-function change for a cleaved Si(111) surface exposed to successive evaporations of Na. It decreases until it reaches the saturation value $\Delta\phi_{\text{sat}} = -2.7$ eV, at 8-min evaporation time. Around half of the saturation coverage (4 min) the LEED pattern transforms from a 2×1 into a 1×1 well-ordered structure. As with K and Cs,^{13,14} we assign the saturation coverage to the completion of the first monolayer. After 2–3 h under measurement conditions the Na-covered Si(111) surfaces showed signs of contamination as monitored by UPS.

The development of the unoccupied electronic states as a function of sodium evaporation is shown in Fig. 2. The bottom spectrum for the clean Si(111) 2×1 surface¹⁵ with the well-known surface state U_1 and bulk conduction-band peaks A and B changes immediately with Na deposition. At first U_1 is quenched, then around $\frac{1}{2}$ -monolayer coverage (4 min) corresponding to the $2 \times 1 \rightarrow 1 \times 1$ transition, a new spectral feature U'_1 starts to grow and move towards the Fermi level. This Na-induced surface state reaches its maximum intensity with the completion of the saturated monolayer (8 min), and compared to the K- or Cs-induced features on Si(111) (cf. Refs. 13 and 14) it has the most intense and pronounced spectral shape of all. Further evaporation causes U'_1 to diminish again. In addition to the occurrence of U'_1 we note a second Na-induced structure denoted U'_2 which seems to split off from the bulk silicon conduction-band peak A and then stays more or less constant in energy and intensity.

The minimum energy position of U'_1 stays 0.6 eV above E_F in contrast to, e.g., the metallic K overlayer¹⁴ with a minimum value of 0.2 eV and a tailing across the Fermi level. This semiconducting behavior for the Na overlayer

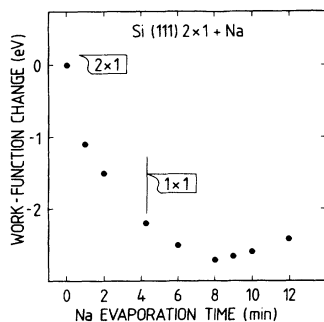


FIG. 1. The change of the work function $\Delta\phi$ as obtained from the onset of the absorption current as a function of Na evaporation time in minutes. The minimum at 8 min is defined as the saturated-monolayer coverage (1 ML). At about half of this coverage (4 min) the LEED pattern changes from the original 2×1 to a 1×1 pattern.

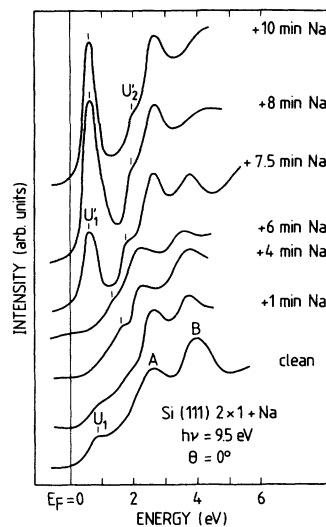


FIG. 2. Normal-incidence inverse photoemission spectra of Na on Si(111) at $h\nu = 9.5$ eV as a function of sodium coverage. The evaporation times correspond to Fig. 1.

is corroborated by UPS measurements (not shown) which do not find any spectral intensity at the Fermi level either. To elucidate the question of metallicity further we have performed angle-resolved IPS and UPS measurements for the saturated monolayer. Only the inverse-photoemission spectra are shown in Fig. 3 for the $\bar{\Gamma}-\bar{M}$

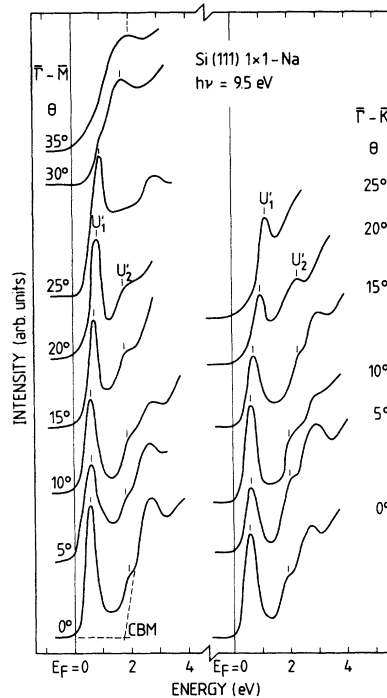


FIG. 3. Angle-resolved inverse photoemission spectra at $h\nu = 9.5$ eV for different incidence angles θ , probing states along the $\bar{\Gamma}-\bar{K}$ azimuth (right panel) and the $\bar{\Gamma}-\bar{M}$ azimuth (left panel) of the Si(111) 1×1 -Na surface Brillouin zone. The tangent drawn in the bottom left spectrum is used to derive a value for the conduction-band minimum (CBM).

(left panel) and the $\bar{\Gamma}$ - \bar{K} azimuth (right panel).

The very pronounced Na surface state U'_1 of Fig. 2 for the saturated monolayer exhibits an upward energy dispersion with increasing polar angle θ , i.e., away from the Fermi level for both azimuthal directions. Along $\bar{\Gamma}$ - \bar{M} we note a broadening of U'_1 for polar angles $\theta \geq 30^\circ$ indicating a possible hybridization with bulk states, as the surface-state band leaves the projected bulk band gap. The second feature U'_2 is no longer discernible at higher angles, while it exhibits little dispersion for the $\bar{\Gamma}$ - \bar{M} azimuth, and an about 1-eV dispersion for the $\bar{\Gamma}$ - \bar{K} azimuth. In fact, only this second Na-induced feature discriminates the two azimuths from each other.

In direct photoemission (not shown) there is also a very pronounced Na-induced surface-state peak S dominating the spectra. For $\theta \geq 15^\circ$ it has a strong downward dispersion for both symmetry directions, but for $\theta < 15^\circ$ its behavior is more complex as it seems to split off from a broader structure with a second less-pronounced peak dispersing to lower energies. Our experimental findings for the saturated-monolayer covered Si(111)1 \times 1-Na surface are summarized in Fig. 4, where the peak positions from IPS in Fig. 3 and UPS (not shown) are plotted as a function of k_{\parallel} , the wave vector parallel to the surface. Clear peaks are shown as full dots with error bars, while weaker features are reproduced as open circles. The unoccupied surface state U'_1 has a parabolic energy dispersion with a minimum at the $\bar{\Gamma}$ point, while the occupied surface state S exhibits a weaker dispersion with shallow minima at \bar{M} and \bar{K} . Clearly this Si(111)1 \times 1-Na surface is semiconducting with an indirect surface band gap.

We have also incorporated in Fig. 4 the calculated bands for comparison. As both existing band-structure calculations^{5,10} are rather symmetric around the $\bar{\Gamma}$ point, we represent the two azimuths separately: along $\bar{\Gamma}$ - \bar{K} we have reproduced the bands from Northrup's calculation⁵ who used the first-principles pseudopotential method in the local-density approximation. He gets $\Delta\phi = -2.7$ eV in perfect agreement with the measured value (see above) and an ionic bonding of the Na 3s to the 3p dangling bonds of the Si surface. Among the various atom configurations total-energy minimization favors⁵ the threefold-hollow site. The latter is in contrast to the calculations by Ossicini, Arcangeli, and Bisi¹⁰ who favor the threefold-filled site with a charge transfer of 0.14 electrons per Na atom indicating a covalent bonding. Their electronic structure results are based on the linear muffin-tin orbital method in the atomic-sphere approximation and are shown in Fig. 4 along the $\bar{\Gamma}$ - \bar{M} azimuth. Since the occupied bands can usually be calculated more accurately than the empty ones, we have shifted each theoretical result in Fig. 4 so that the measured and calculated occupied surface-state bands coincide best. This results in the discontinuities in the projected bulk bands (hatched areas in Fig. 4) at the $\bar{\Gamma}$ point between the two different calculations.

On the other hand, the calculated empty surface-state bands do not differ substantially from the measured bands either. This is surprising as in most cases the calculated surface-state band gaps are much smaller than

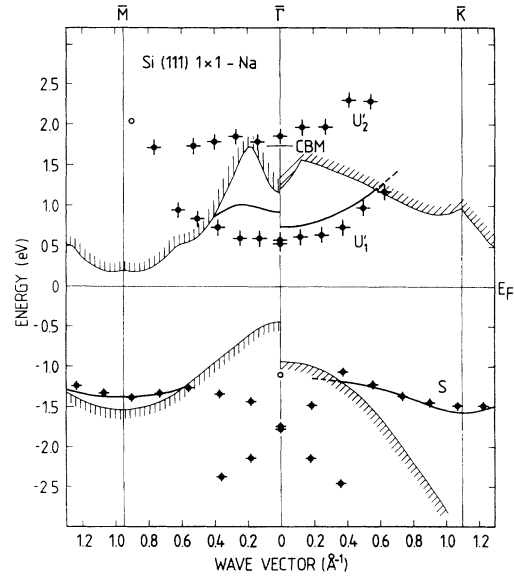


FIG. 4. The energy dispersion $E(k_{\parallel})$ of the empty and occupied surface-state features of 1-ML Na on Si(111)1 \times 1-Na as measured by angle-resolved IPS (Fig. 3) and UPS (not shown), respectively. The crosses indicate the estimated uncertainties. Along $\bar{\Gamma}$ - \bar{K} (right side) we compare to the calculated bands of Northrup (Ref. 5), along $\bar{\Gamma}$ - \bar{M} (left side) to those of Ossicini, Arcangeli, and Bisi (Ref. 10). The theoretical surface-state bands have been adjusted in energy to give best agreement for the occupied part. The hatched area represents the projected bulk bands of each calculation.

measured band gaps unless the self-energy contribution is properly included.¹⁶ Since the self-energy involves the effects of exchange and correlation on the single-particle excitation energies, it implies that these effects must be rather small or be compensated for by other energy contributions as, e.g., hybridization energies since the surface bands are close to projected bulk bands.

We have already noted above that the broadenings of the otherwise sharp surface features S and U'_1 indicate the mixing with bulk states near the edges of the projected bulk band gap. In Fig. 4 this is now directly evident, as the occupied as well as the empty surface states become surface resonances near the $\bar{\Gamma}$ point and halfway along $\bar{\Gamma}$ - \bar{M} and $\bar{\Gamma}$ - \bar{K} , respectively. The downward dispersion of S , as soon as it has become degenerate with projected bulk states near the $\bar{\Gamma}$ point, is not corroborated by either of the two calculations, while a weak structure shown as an open circle at the $\bar{\Gamma}$ point in Fig. 4 may reflect the top of the valence band. The splitting off and downward dispersion of a second occupied state measured by UPS cannot be explained by the calculations.^{5,10} Although we believe that the agreement with respect to the occupied surface-state bands is very good for both theories, we cannot—based on UPS alone—discriminate between the two calculations. Their primary and contrasting conclusions were ionic bonding and threefold-hollow site as the Na adsorption position⁵ versus covalent bonding and threefold-filled site.¹⁰

Focusing upon the unoccupied states and our inverse-photoemission results we can conclude that the width

and spectral shape of Northrup's surface-state band agrees well with the measured dispersion of U'_1 (cf. Fig. 4), whereas the calculated band favoring a covalent bonding¹⁰ is too flat and has a more concave, nonparabolic shape as opposed to the parabola-shaped U'_1 band with a total width of 0.7 eV. Hence we conclude that at least among these two calculations^{5,10} the ionic-bonding picture with the total charge transfer of the Na 3s electron is supported by our measurements. This is also consistent with the proper determination⁵ of the work-function reduction of $\Delta\phi_{\text{sat}} = -2.7$ eV, and implies that the Na adsorption position is the threefold-hollow site.

Recently, *ab initio* molecular-dynamics simulations using a plane-wave expansion for the electron wave functions have been performed,¹⁷ which use simulated annealing techniques to determine the equilibrium structure. The lowest energy configuration also yields the 1×1 surface structure with the threefold-hollow site as the most stable one. The calculated corresponding surface-state dispersions agree almost perfectly with our measured dispersions. However, the bonding character differs from Northrup's ionic result as discussed elsewhere.¹⁷

In Fig. 3 we have tried to derive the conduction-band minimum (CBM) by drawing a tangent to the bulk feature *A*. In this way we derive the CBM to be 1.7 eV above the Fermi level (see Fig. 4). It follows that the second empty feature U'_2 lies practically above the CBM and must be degenerate with bulk states over the k_{\parallel} regime measured. This higher-lying band is not reproduced in either of the calculations.^{5,10} It may reflect an interface state as it splits off from the silicon bulk feature *A* in Fig. 2 as a function of Na coverage. This means its charge density is mainly centered between the sodium overlayer and the silicon substrate, in contrast to a surface state with a charge density restricted to the top surface layer. Energetically U'_2 is 1.3 eV above U'_1 which

would be consistent with Na 3d derived states as calculated by Wimmer¹⁸ for a free-standing hexagonal monolayer of sodium. Such *d* character with a nonisotropic wave function is also consistent with the observed different dispersion behavior for the two azimuthal directions: almost flat band along the $\bar{\Gamma}-\bar{M}$ and upward for the $\bar{\Gamma}-\bar{K}$ direction (cf. Fig. 4). Future theoretical work is necessary in order to clarify the nature of this high-lying Na induced band.

Finally, in comparison to the Si(111) 1×1 -Na surface, the Si(111) 2×1 -K surface¹⁴ does not induce any surface structural transitions, it is metallic over a broad coverage regime, and the metallization occurs by a filling of the Si surface-state band in agreement with the ionic-bonding picture.⁴ The Si(111) $\sqrt{3} \times \sqrt{3}R30^\circ$ -Cs surface¹³ has this peculiar surface structural transition, and is semiconducting. Since there are no calculations yet, we cannot answer the question of ionic-versus-covalent bonding for the Cs case. But we note that for Na and Cs (Ref. 19) and K (Ref. 20) on the Si(100) 2×1 surface a covalent bonding picture is generally favored.

In conclusion we state that the alkali metals do not behave isoelectronically on the same silicon surface, and that the same alkali metal may be characterized by different bonding properties on the 2×1 surface of Si(111) or of Si(100). We believe that the increasing competition between the alkali-metal-semiconductor and the alkali-metal-alkali-metal interaction as a function of coverage may be the reason, as both are dependent on the atomic radii and polarizabilities of the alkali-metal atoms.

We thank M. Tschudy for his competent assistance with all experiments, and W. Andreoni, I. Moullet, and M. Parrinello for sharing their Na/Si(111) results prior to publication.

*Corresponding author, electronic address: BITNET, BRL@ZURLVM1.

†Present address: Department of Synchrotron Radiation Physics, University of Lund, S-22362 Lund, Sweden.

‡Present address: Fraunhofer Institut für Mikrostrukturtechnik, Margrete-Steiff-Weg 3, D-2210 Itzehoe, Germany.

§Present address: ABB HV Switchgear AB, S-77180 Ludvika, Sweden.

¹N. J. DiNardo, *et al.*, Phys. Rev. Lett. **65**, 2177 (1990).

²L. J. Whitman, *et al.*, Phys. Rev. Lett. **66**, 1338 (1991).

³K. O. Magnusson and B. Reihl, Phys. Rev. B **40**, 7814 (1989).

⁴S. Ciraci and I. P. Batra, Phys. Rev. Lett. **56**, 877 (1986); **58**, 1982 (1987).

⁵J. E. Northrup, J. Vac. Sci. Technol. A **4**, 1404 (1986).

⁶I. P. Batra and S. Ciraci, Phys. Rev. B **37**, 8433 (1988).

⁷R. Ramirez, Phys. Rev. B **40**, 3962 (1989).

⁸H. Ishida, K. Terakura, and M. Tsukada, Solid State Commun. **59**, 356 (1986).

⁹H. Ishida and K. Terakura, Phys. Rev. B **40**, 11 519 (1989).

¹⁰S. Ossicini, *et al.*, Phys. Rev. B **42**, 7671 (1990).

¹¹Y. Ling, *et al.*, Phys. Rev. B **39**, 10 144 (1989).

¹²T. Kato, *et al.*, Surf. Sci. **209**, 131 (1989).

¹³K. O. Magnusson and B. Reihl, Phys. Rev. B **39**, 10 456 (1989).

¹⁴B. Reihl and K. O. Magnusson, Phys. Rev. B **42**, 11 839 (1990).

¹⁵B. Reihl, K. O. Magnusson, J. M. Nicholls, P. Perfetti, and F. Salvan, in *Metallization and Metal-Semiconductor Interfaces*, Vol. 195 of *NATO Advanced Study Institute Series B: Physics*, edited by I. P. Batra (Plenum, New York, 1989), p. 397.

¹⁶J. E. Northrup, M. S. Hybertsen, and S. G. Louie, Phys. Rev. Lett. **66**, 500 (1991).

¹⁷I. Moullet, W. Andreoni, and M. Parrinello, following paper, Phys. Rev. B **46**, 1842 (1992); (unpublished).

¹⁸E. Wimmer, J. Phys. F **13**, 2313 (1983).

¹⁹P. Soukiassian, *et al.*, Surf. Sci. **221**, L759 (1989).

²⁰T. Kendelewicz, *et al.*, Phys. Rev. B **37**, 7115 (1988).